Urbanization Drives SOC Accumulation, Its Temperature Stability and Turnover in Forests, Northeastern China

Chang Zhai [1,2], Wenjie Wang [1,3], Xingyuan He [1,*], Wei Zhou [1,3], Lu Xiao [3] and Bo Zhang [3]

[1] Key Laboratory of Wetland Ecology and Environment, Northeast Institute of Geography and Agroecology, Chinese Academy of Sciences, Changchun 130102, China; zhaichang@iga.ac.cn (C.Z.); wangwenjie@iga.ac.cn (W.W.); bsstzw@163.com (W.Z.)

[2] University of Chinese Academy of Sciences, Beijing 100049, China

[3] Key Laboratory of Forest Plant Ecology, Northeast Forestry University, Harbin 150040, China; xiaolu1212@foxmail.com (L.X.); w9426426@163.com (B.Z.)

[*] Correspondence: hexingyuan@iga.ac.cn; Tel.: +86-431-8554-2277

Abstract: Global urbanization is a vital process shaping terrestrial ecosystems but its effects on forest soil carbon (C) dynamics are still not well defined. To clarify the effects of urbanization on soil organic carbon (SOC) variation, 306 soil samples were collected and analyzed under two urban–rural gradients, defined according to human disturbance time and ring road development in Changchun, northeast China. Forest SOC showed a linear increase with increasing human disturbance time from year 1900 to 2014 (13.4 g C m^{-2} year^{-1}), and a similar trend was found for the ring road gradient. Old-city regions had the longest SOC turnover time and it increased significantly with increasing urbanization (p = 0.011). Along both urban–rural gradients SOC stability toward temperature variation increased with increasing urbanization, meaning SOC stability in old-city regions was higher than in new regions. However, none of the urban–rural gradients showed marked changes in soil basal respiration rate. Both Pearson correlation and stepwise regression proved that these urbanization-induced SOC patterns were closely associated with landscape forest (LF) proportion and soil electrical conductivity (EC) changes in urban–rural gradients, but marginally related with tree size and compositional changes. Overall, Changchun urbanization-induced SOC accumulation was 60.6–98.08 thousand tons, accounting for 12.8–20.7% of the total forest C biomass sequestration. Thus, China's rapid urbanization-induced SOC sequestration, stability and turnover time, should be fully estimated when evaluating terrestrial C balance.

Keywords: urbanization; forest soil organic carbon; soil basal respiration; temperature stability; carbon turnover; global change

1. Introduction

Urbanization constitutes an important land use and land cover change process, with impacts on both terrestrial and aquatic carbon pools, and understanding and quantifying carbon flows in cities offers a powerful lens into urban ecosystems and provides a compact metric of urban sustainability [1]. In China, the urbanization rate increased from 17.92% in 1978 to 51.27% in 2011 and the population in city areas has risen from 0.17 billion to 0.69 billion [2], exceeding 50% of China's total population. A science research agenda grounded in sustained and intense observations, focusing on a statistically significant sampling of cities, is crucial for estimating urban carbon pools and fluxes as well as the processes controlling them, and will increase our understanding of the carbon cycle [1]. Soil is

the largest terrestrial organic carbon pool, containing twice as much carbon as the atmosphere or vegetation before its release into the atmosphere, and forests are the largest terrestrial ecosystem for carbon sequestration [3]. A small change in soil carbon may radically alter the balance of terrestrial ecosystems and the global carbon cycle [4]. It is important to scientifically understand the effects of urbanization on forest carbon dynamics, especially the underground soil organic carbon (SOC) changes and underlying mechanisms related with soil turnover, temperature stability and respiration.

Urbanization effects are typically evaluated along urban–rural gradients, which have been used in studies considering ecosystem structure [5], biodiversity [6], and forest soil heavy metals [7]. In a city with clear development history, classification of regions with urban settlement history could be used as urban–rural gradients with exact development time. In China, cities are usually sprawled through ring road development, i.e., a first ring road region will have had the longest urbanization history, while an outer ring road will have had a shorter urbanization time. On the other hand, ring roads are much more related with lifestyle and government regulations as a sign of urbanization. It is well known among citizens that many government regulations are issued depending on the ring road numbers. In Changchun city, for example, the use of fireworks is now strictly prohibited within the 4th ring road since the government's 16th executive meeting. Also, heavy-polluting vehicles are now forbidden within the 4th ring road from 6 a.m. to 8 p.m. since 1 January 2015. Both two urban–rural gradients related to urban history and ring road-sprawl have been used in the analysis of aboveground biomass [8,9], however, their reliability on SOC changes still needs to be testified in a study. Laboratory experiments set to determine soil basal respiration can also indicate SOC decomposability and turnover [10], and the factor by which soil respiration rate increases when temperature increases 10 °C (Q_{10}) can indicate the temperature stability of SOC decomposition [11]. Thus, besides the SOC concentration and density, soil respiration, temperature stability and turnover time in urban soils are important for understanding the underlying mechanisms related to SOC changes [5,10,12]. Furthermore, forest SOC has been mostly considered a constant or a null value in evaluating the response to urbanization [13–16], although some studies have shown possible accumulations [8,9,17] or releases [18]. Based on a systematic study and a large dataset in a typical fast-urbanized city, scaling-up of forest SOC changes to a city level will facilitate awareness of underground forest SOC importance in urbanization processes.

Reasons for underground SOC changes have been ascribed to land use changes [13], tree species alternation [19] and tree size differences, as well as soil properties [13]. In urban regions of China, a forest is defined as the trees, mainly arbors (groves), in and around the cityscape which reach a certain scale and coverage [20], and forest types are usually classified as roadside forest (RF), ecological welfare forest (EF), landscape forest (LF), and affiliated forest (AF), according to their land use differences [20]. Alternations in land uses possibly contribute to SOC dynamics to some extent [21], while tree species also differ in SOC accumulation and the potential turnover owing to litter quality [19]. Moreover, tree dimensions including diameter, height and crown size are also responsible for SOC variations, owing to tree size being a proxy for forest development (tree age). Also, soil properties themselves including pH, bulk density (BD) [22] and electrical conductivity (EC) could regulate soil microbes and thus SOC dynamics [23,24]. These factors are the main reasons for changes in forest SOC, soil respiration, temperature stability and turnover during urbanization processes. Furthermore, in a large-scale field survey, a proper statistical method facilitates clarification of the complex interaction of multiple factors on the response function [25]. An integrated approach including correlation analysis and regression analysis [22] can be used to obtain reliable results and explanations of such variations.

For addressing the urbanization effects on forest SOC changes, in this study we assessed the influence of urbanization on SOC accumulation, its turnover and temperature stability, and analysed the potential reasons for such variations. Specifically, we addressed the following questions: (1) how much does SOC density (SOCD), soil basal respiration, temperature stability, and carbon turnover change along urban–rural gradients? (2) Did human disturbance time-related gradients and ring road-related gradients produce a similar result? And (3) what is the possible reason for these SOC

urban–rural patterns? Are there any implications for future studies and forest management? Under a global urbanization background and especially considering China's fast urbanization in recent years, addressing these questions might allow for evaluating its forests' ecological services.

2. Materials and Methods

2.1. Study Area Description and Urbanization Level Classification

Our study was conducted in Changchun, a typical medium-sized city, which is the capital of Jilin province, northeast China (43°42′ to 44°03′ N, 125°09′ to 125°27′ E). Covering approximately 524 km² (within the beltway) (Figure 1), Changchun had 3.659 million inhabitants at the end of 2014 (Changchun Statistical Bureau data). The climate is temperate humid or sub-humid continental monsoon, the mean annual precipitation is 567 mm, and the mean air temperature is 4.8 °C [26]. Dominant soil types are black soil, dark-brown soil, and chernozem [27].
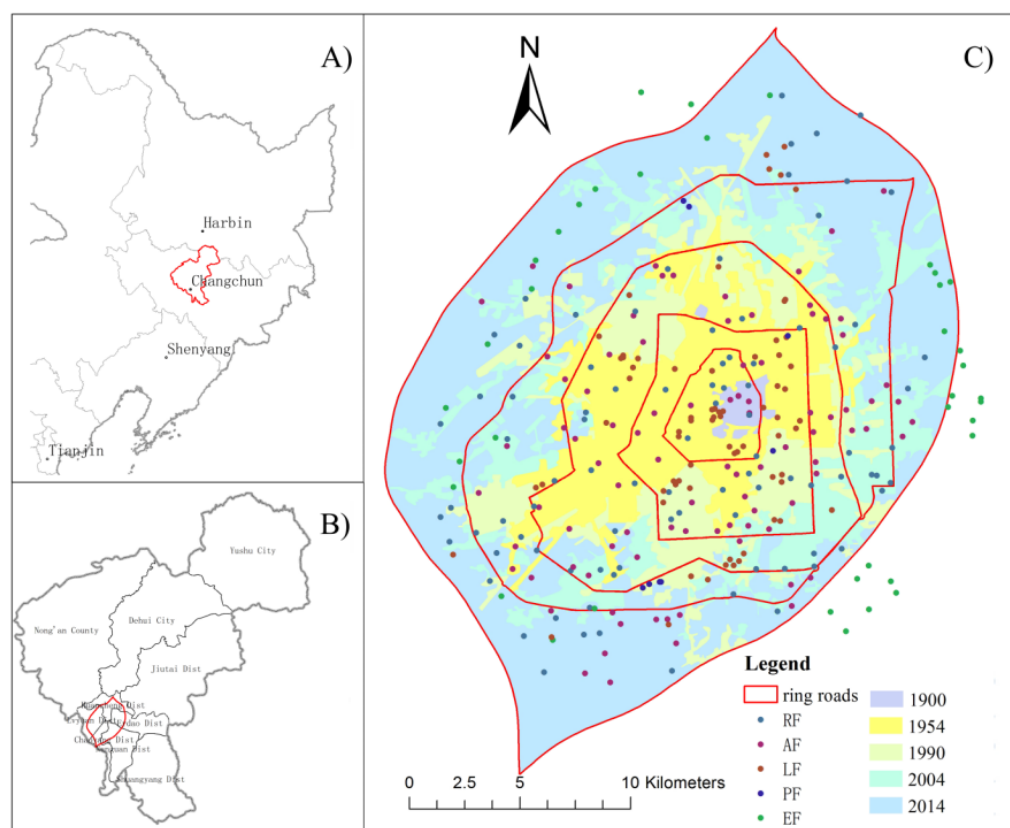

Figure 1. The location and samples of the study area. Notes: (**A**) Northeast China; (**B**) Changchun administrative region; and (**C**) map of study area, in which the shading represents the regions of different soil build-up time, the red lines indicate the different ring road boundaries and the dots are the sample points of different forest types: RF, roadside forest; AF, affiliated forest; LF, landscape and relaxation forest; EF, ecological and public welfare forest; and PF, production and management forest (the map was created by ArcGIS 10.3, Esri, RedLands, CA, USA).

We used human disturbance time and ring roads to represent the urbanization level. Changchun historical maps and literature data [28] were used to distinguish human disturbance times. Five categories, based on the years at which soil was built-up (the years 1900, 1954, 1990, 2004, and 2014), indicated human disturbance time, i.e., 114, 60, 24, 10, and 0 years, respectively. Moreover, ring road numbers are another symbol to indicate the urbanization degree, which studies have shown can be used as a proxy for the degree of urbanization [29] or urban–rural gradients [21,27]. Accordingly, the urban

area was divided into five categories, i.e., 1st, 2nd, 3rd, 4th, and 5th ring road regions (Figure 1). For understanding urbanization effects, the urban–rural gradient transect method is generally used to evaluate time and space substitutions. However, the choice of this transect is subjective and usually biases the urbanization level determined. The large urban dataset used in the present paper, as well as the use of an urban–rural gradient related to ring road development and urban disturbance time, help contribute to a more objective determination of the urbanization level, also reflecting the real urbanization process.

2.2. Soil Sampling, Field Survey and Tree Measurement

Spot 5 (Earth observation satellite system launched by France) image data collected on 14 September 2010 were geo-rectified and re-projected in ArcGIS firstly. Then, urban forest locations were extracted from the image by the visual interpretation method (ArcGIS). The 306 sites in the present study (12 for 114 years, 90 for 60 years, 57 for 24 years, 41 for 10 years, 106 for 0 years; 31 in the 1st ring road, 55 in the 2nd ring road, 75 in the 3rd ring road, 50 in the 4th ring road, and 95 in the 5th ring road, respectively) were sampled according to the stratified random sampling method to allocate plot numbers [30] based on their locations and forest coverage (Figure 1).

Field surveys were conducted in July and August 2014, and each plot was about 400 m^2 for tree measurement and soil sampling. At each site, four replicate soil samples were taken undisturbed under the trees down to 20 cm, using a cutting ring (a soil container, 100 cm^3). The ring-cup was inserted into the soil with a plastic hammer. Then, the intact soil with 100 cm^3 was taken out, and the samples were collected in cloth pockets, transported to the laboratory, and then mixed and fully air-dried at least 2 months until a constant weight for bulk density measurement. Visible plants, stones and rock fragments, and roots greater than 2 mm were removed from soil samples [9] before they were ground and sieved (0.25 mm mesh) for laboratory analysis. For testing purposes, air-dried samples are usually 1% different from oven-dried (105 °C) soil, and thus utilization of air-dried samples did not bias the total SOC determination.

At the same time of soil sampling, all tree species were recorded according to tree name (genus, family) and leaf morphology (conifer and broadleaf). Diameter at breast height (DBH), tree height (TH), height under branch (HUB), and crown size (CS) of each tree in the plot were also recorded. DBH was measured at 1.3 m above-ground level by a DBH tape. TH and HUB were measured using a Nikon Forestry PRO550 laser rangefinder (Nikon, Jackson, MS, USA). Canopy projection was measured on the ground by a regular long steel tape in two directions (North–South; East–West), and these data were used to calculate the CS with the ellipse area formula. These compositional data and tree size data were used to find their possible contribution to SOC patterns in urban–rural gradients.

Different land use usually accompanies different SOC dynamics. For finding different forest uses contributing to the urban–rural SOC patterns, the field survey also recorded the forest into five types [20] based on their location, function, and management objectives: (1) roadside forest (RF), trees along railroads, highways, boulevards, roads, and streets; (2) affiliated forest (AF), trees next to buildings in school yards, campuses, hospitals, commercial and business districts, industrial areas and residential areas; (3) landscape and relaxation forest (LF), trees in the public parks, forest parks, historic sites, and scenic areas; (4) ecological and public welfare forest (EF), trees next to river banks and farmlands; and (5) production and management forest (PF), trees in the nurseries, orchards, plantations, and woodlands.

2.3. SOC, Basal Respiration, Q$_{10}$, Turnover and Soil Properties: Laboratory Analysis and Parameter Computation

Soil organic carbon was measured by the heated dichromate/titration method [31]. In this procedure, potassium dichromate ($K_2Cr_2O_7$) and concentrated H_2SO_4 were added to soil subsamples (0.1 to 0.5 g). Solutions were fully mixed and halted overnight, and tubes were then immersed in an auto-controlled 170–180 °C oil bath for 5 min. These digestion solutions were titrated with a $FeSO_4$ solution with an exact concentration, using two to three drops of phenanthroline as a colour

indicator (brick-red indicated the endpoint of the titration). Soil samples and a standard soil sample (ASA1, Institute of Geophysical and Geochemical Exploration, Langfang, China) were measured simultaneously in each digestion, and the final SOC content obtained for the reference/standard soil sampled assumed digestion was complete [5]. A 1:5 soil solution (one part soil to five parts distilled water) was used to determine soil pH with an acidity meter (Sartorius PT-21, Shanghai, China). Soil electrical conductivity (EC) was determined with an EC meter (DDS-307, Shanghai Precision Scientific Instruments Co., Ltd., Shanghai, China). Topsoil SOCD (kg/m^2) within each sample was calculated according to Equation (1) [32]:

$$SOCD = BD \times C \times (1 - \delta) \times h \tag{1}$$

where BD is the bulk density (g/cm^3), C is the SOC content (g/kg), δ is the fraction of gravel material, and h is the topsoil depth (0.2 m).

Soil basal respiration in laboratory measurement was carried out in the following manner. Dry soil subsamples (100 g) from each of the 306 samples were incubated in two petri dishes (9 cm diameter) under three temperature grades in 3 growth cabinets (HPG-280 HX, Donglian Company, Harbin, China) [33]. Soil subsamples were adjusted to 80% WHC (water-holding capacity) and pre-incubated for seven days at 20 °C to minimize the initial flush of soil respiration, and then transferred to constant temperature and humidity incubators at 10, 20, and 30 °C for seven days (a pre-test before the experimental proceedings found that after 5 days of incubation, the soil basal respiration rate was almost steady from day 6 (supplemental Table S1)). Soil basal respiration rates were then measured using a LI-6400 meter (LI-COR, Inc., Nebraska, NE, USA), inserting the sensor head into the incubator and above the petri dishes to improve measurement precision (supplemental Figure S1). Water loss during incubation was examined gravimetrically every day, and it did not exceed 2%.

The relationship between temperature and soil respiration was modelled according to the Van't Hoff equation [34].

$$R = R_0 e^{bT} \tag{2}$$

where R is the above-mentioned soil basal respiration rate (SR) ($\mu mol/m^2/s$), R_0 is a fitting parameter referring to soil respiration rate at 0 °C, T is the air temperature which was 10 °C, 20 °C, 30 °C respectively, and b is a parameter defining temperature dependence upon soil respiration.

Temperature sensitivity (Q_{10}) of SOC respiratory decomposition was calculated as the following equation [34]:

$$Q_{10} = e^{10b} \tag{3}$$

The SOC turnover time (TT) τ (years) can be calculated from the total reservoir size (C_{total}, $kg\ C\ m^{-2}$) and the influx or the outflux ($kg\ C\ m^{-2}\ year^{-1}$) as the Equation (4) [35]. In this study, the total reservoir size was the carbon stock in soils (SOCD, kg/m^2), the influx was the carbon uptake through gross primary production (GPP), which we did not consider under the laboratory measurement, and the outflux was the carbon losses, which were represented as the soil annual respiration (AR, $kg/m^2/year$) (heterotrophic respiration, in this paper).

$$\tau = C_{total}/flux \tag{4}$$

Soil C efflux from AR was calculated according to Function (2) by using whole-year hourly air temperature data (acquired from Changchun Meteorological Station). A total of 20 stations distributed in urban–rural gradients were used in this scaling-up. We made use of inverse distance weight interpolation in ArcGIS 10.3 to obtain the air temperature of the 306 plots, and calculated the soil respiration flux by multiplying the forest soil area and the mean soil respiration rate of the 306 plots. The air temperature data were divided into each gradient in the ring road and urban disturbance time-related urban–rural gradients. This kind of respiration scaling-up included the temperature differences in downtown regions and outskirts to help ensure data reliability.

The carbon accumulation due to human disturbance time and ring road-related urbanization were calculated by multiplying the areas of different urbanization gradients and the C accumulation rate. Within this analysis, the areas were derived from the remote sensing image, and the rate of C accumulation equalled the slope of the regression equation of the two urbanization gradients. We calculated the total soil carbon sequestration content at 1-m depth and compared it with the aboveground C biomass. According to previously published data, SOCD at 0–20 cm depth is approximately 50% of that obtained at 0–100 cm depth in China [36–38].

2.4. Forest Type, Tree Composition, Soil Properties and Tree Size Properties: Urban–Rural Gradient Analysis

For finding the underlying reasons for SOC urban–rural patterns, the forest type changes, compositional changes, soil properties and tree size were analysed according to the field survey data. In each of the 5 human disturbance time gradients and 5 ring road gradients, all sampling plots were averaged for calculating tree dimensions (DBH, TH, HUB, CS) and soil properties (bulk density, EC and pH). In the case of forest type, the proportion of RF, AF, LF, EF and PF types to total sampling plots was calculated in each urban–rural gradient for finding relative changes of forest types at urban–rural gradients.

In the case of compositional changes, we divided the trees according to their family. A total of 7 categories were classified according to field survey data, as follows. Category 1: Betulaceae included 2 species—*Betula platyphylla* and *Betula costata*. Category 2: Aceraceae included 4 species—*Acer mono*, *Acer negundo*, *Acer palmatum* and *Acer mandshuricum*. Category 3: Rosaceae included 9 species—*Armeniaca mandshurica*, *Malus baccata*, *Padus maackii*, *Padus racemosa*, *Prunus ussuriensis*, *Pyrus ussuriensis*, *Crataegus pinnatifida*, *Amygdalus davidiana* and *Prunus ceraifera* f. *atropurpurea*. Category 4: Pinaceae included 7 species – *Pinus sylvestris* var. *mongolica*, *Pinus tabuliformis*, *Pinus tabulaefomis* var. *mukdensis*, *Larix gmelinii*, *Pinus banksiana*, *Abies nephrolepis* and *Picea koraiensis*. Category 5: Salicaceae included 5 species – *Salix babylonica*, *Salix matsudana*, *Populus alba*, *Populus davidiana* and *Populus cathayana*. Category 6: Ulmaceae included 3 species—*Ulmus pumila*, *Ulmus pumila* f. *tenue* and *Ulmus pumila* cv. *jinye*. Category 7 were recorded as other spp., and included 6 species – *Albizia kalkora*, *Catalpa ovate*, *Fraxinus mandshurica*, *Quercus mongolica*, *Rhus typhina* and *Phellodendron amurense*. Similar to forest types, the proportion of 7 categories of family and 2 groups of conifer/broadleaf in each gradient was calculated as the ratio between plot numbers including this family and total surveyed plots.

2.5. Statistical Analyses

We used multivariate analysis of variance (MANOVA) followed by Duncan multiple comparisons tests to evaluate the differences in SOCD, SR (average basal soil respiration rate at three temperature grades), Q_{10}, and TT among different human disturbance times, ring roads and the interaction between them. Regression analysis was used to describe the relation of two urban–rural gradients with SOCD, SR, Q_{10}, and TT. Significant linear relations indicated evident urbanization-induced SOC-related changes.

For finding the possible contribution of forest type, tree composition, soil properties and tree size differences to the urban–rural gradient patterns of soil carbon, two statistical analyses including Pearson correlation analysis and stepwise regression analysis were used in this paper. All statistical analyses were performed using SPSS Statistics 21.0 (IBM, Armonk, NY, USA).

3. Results

3.1. Effect of Urban–Rural Gradients on Soil Carbon Dynamics: MANOVA Results and Interactions

MANOVA results (Table 1) show that SOCD, SR, Q_{10}, and TT differed among two urban–rural gradients related to human distance time ($p < 0.05$) and ring road ($p < 0.01$). However, there was no significant interaction between human distance time and ring road ($p > 0.05$).

Using the *F*-value as an indicator of the magnitude of the effects of both urban–rural gradients, SOCD and TT were most affected by human disturbance time (7–31% higher *F*-values) while SR and Q_{10} were most affected by ring roads (51–55% higher *F*-values).

Table 1. MANOVA results of urban–rural gradients on soil organic carbon (SOC)-related properties in forest soil of Changchun city of China.

Independent Factors	*F* or *p* Values	SOCD	SR	Q_{10}	TT
Human disturbance time	*F*-value	8.32 *	2.71 *	2.45 *	6.01 *
	p-value	0.000 *	0.030 *	0.047 *	0.000 *
	df	4	4	4	4
Ring road urban–rural gradient	*F*-value	7.78 *	4.20 *	3.71 *	4.60 *
	p-value	0.000 *	0.003 *	0.006 *	0.001 *
	df	4	4	4	4
Human disturbance time × Ring road urban–rural gradient	*F*-value	0.36	0.65	0.52	0.35
	p-value	0.939	0.735	0.843	0.946
	df	8	8	8	8

Note: * indicates significant influences of urbanization. SOCD, soil organic carbon density; SR, soil basal respiration rate; and TT, turnover time.

3.2. Influence of Human Disturbance Time on SOCD, SR, Q_{10} and TT: Magnitude and Regression Analyses

Figure 2 shows the magnitude of these differences in SOCD, SR, Q_{10} and TT. The highest SOCD, SR, and TT and the lowest Q_{10} were found in the oldest urban region, i.e., in the region with 114 years of human disturbance. Linear regression analyses showed a significant increase in SOCD and TT with increasing human disturbance time ($R^2 > 0.91$, $p < 0.05$), while a linear and significant decrease was found in Q_{10} ($R^2 = 0.87$, $p = 0.038$).
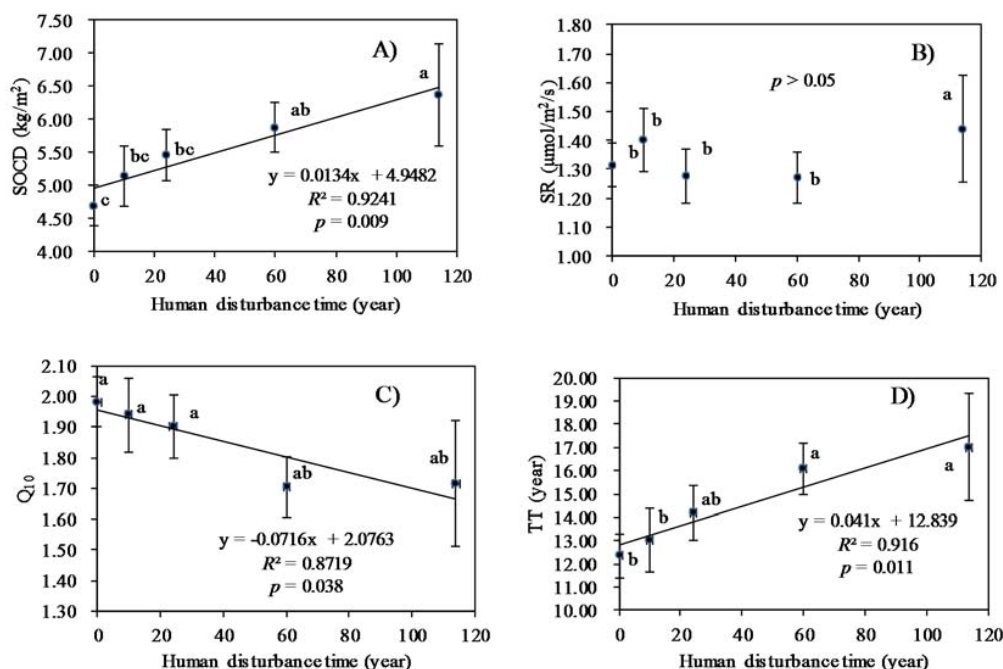

Figure 2. Human disturbance time influences on (**A**) SOCD; (**B**) SR; (**C**) Q_{10} and (**D**) TT, in forest soil of Changchun city of China. Notes: SOCD, soil organic carbon density; SR, soil basal respiration rate; and TT, turnover time. Error bars showed standard deviation, and lowercase letters indicate significant differences based on the MANOVA test statistics. The same letters indicate no significant differences, and different letters indicate significant differences ($p < 0.05$).

The disturbance time-related variations in SOCD, SR, Q_{10} and TT were 1.54-, 1.35-, 1.23-, and 1.38-fold, respectively. Considering the significant linear slopes of their regression analyses as the changing rate, SOCD accumulated 13.4 g C m^{-2} year^{-1}, Q_{10} decreased 0.076 year^{-1}, and TT increased 0.041 year^{-1} (Figure 2).

3.3. Influence of Ring Road Development on SOCD, SR, Q_{10} and TT: Magnitude and Regression Analyses

Significant differences in SOCD, SR, Q_{10} and TT were found among the 5 ring roads (Figure 3). A linear increase in SOCD was found from the 5th to the 1st ring road, whereas Q_{10} presented the opposite trend; such linear relationships were not found for SR and TT. Linear regression analyses showed a significant increase in SOCD ($R^2 = 0.80$, $p = 0.025$) and a significant decrease in Q_{10} soil temperature stability ($R^2 = 0.84$, $p = 0.028$) with increasing ring road development.
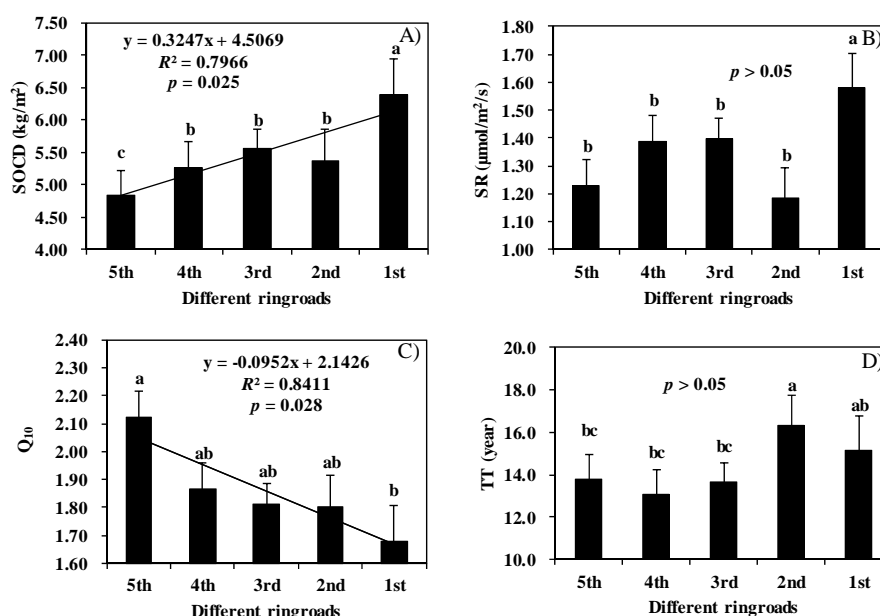

Figure 3. Ring road-related urban–rural gradient influences on (**A**) SOCD; (**B**) SR; (**C**) Q_{10} and (**D**) TT, in forest soil of Changchun city of China. Notes: SOCD, soil organic carbon density; SR, soil basal respiration rate; and TT, turnover time. Error bars showed standard deviation, and lowercase letters indicate significant differences based on the MANOVA test statistics. The same letters indicate no significant differences, and different letters indicate significant differences ($p < 0.05$).

The variations in ring road-related SOCD, SR, Q_{10} and TT were 1.54-, 1.35-, 1.23-, and 1.36-fold, respectively. Considering significant linear slopes as the changing rates, the SOCD in the inner ring road region increased 324.7 g C m^{-2} whereas the Q_{10} value dropped 0.095 with the development of each outward ring road.

3.4. Urban–Rural Gradient Changes in Forest Type, Tree Compostion, Soil Properties and Tree Sizes

RF, AF and LF existed in all urban–rural gradients, but PF did not appear in the city centre and EF was only located in outskirts. The proportion of LF showed a significant increasing trend with the human disturbance time-related urban–rural urbanization gradients ($y = 0.0015x + 0.2094$, $R^2 = 0.538$, $p < 0.05$) as well as the ring road-related urban–rural gradients ($y = -0.109x + 0.617$, $R^2 = 0.837$, $p < 0.05$). However, except LF, other types did not show linear changes in the two urban–rural gradients (Table 2).

As for tree composition (Table 2), except Ulmaceae, all other species existed in all the urban–rural gradient zones. Tree family-based tree species did not display a monotonic changing trend either in human disturbance time-related or ring road-related urban–rural urbanization gradients. In the case

of conifer and broadleaf classification, the proportions of broadleaf trees to conifers were all greater in the two urban–rural gradients.

Table 2. Urban–rural gradient changes in forest type proportion, tree composition proportion, soil properties and tree sizes, in Changchun city, China.

Types	Human Disturbance Time-Related Gradients					Ring Road-Related Gradients				
	114 Year	60 Years	24 Years	10 Years	0 Year	1st	2nd	3rd	4th	5th
Forest Types										
RF	0.25	0.28	0.32	0.39	0.26	0.29	0.16	0.36	0.36	0.28
AF	0.42	0.33	0.35	0.37	0.21	0.19	0.35	0.4	0.4	0.18
LF	0.33 *	0.38 *	0.28 *	0.24 *	0.13 *	0.52 *	0.45 *	0.24 *	0.08 *	0.16 *
PF	0	0.01	0.05	0	0.04	0	0.04	0	0.12	0.38
EF	0	0	0	0	0.36	0	0	0	0.04	0
Compositional differences										
Betulaceae	0.08	0.04	0.04	0.15	0.11	0.10	0.07	0.04	0.06	0.13
Aceraceae	0.08	0.04	0.09	0.05	0.02	0.03	0.07	0.05	0.02	0.04
Rosaceae	0.08	0.24	0.28	0.32	0.15	0.06	0.22	0.40	0.28	0.11
Pinaceae	0.17	0.26	0.26	0.15	0.18	0.39	0.29	0.11	0.28	0.16
Salicaceae	0.25	0.28	0.19	0.22	0.39	0.26	0.22	0.21	0.26	0.42
Ulmaceae	0.17	0.01	0.07	0	0.08	0.06	0.04	0.07	0.02	0.05
Other spp.	0.17	0.12	0.07	0.12	0.08	0.10	0.09	0.12	0.08	0.09
Conifer	0.17	0.24	0.25	0.15	0.18	0.35	0.29	0.11	0.26	0.16
Broadleaf	0.83	0.76	0.75	0.85	0.82	0.65	0.71	0.89	0.74	0.84
Soil properties										
BD (g/cm^3)	1.38	1.39	1.36	1.39	1.38	1.37	1.38	1.38	1.36	1.38
pH	8.03	7.84	7.73	7.99	7.76	7.62	7.69	7.93	8.02	7.82
EC (µs/cm)	182.9 *	145.0 *	112.6 *	116.8 *	99.2 *	165.0 *	131.6 *	125.3 *	123.0 *	95.9 *
Tree size properties										
DBH (cm)	17.06	16.73	15.65	17.15	16.95	19.49	16.22	14.74	16.01	17.85
TH (m)	8.84	7.98	7.33	7.89	7.97	10.17	7.28	7.02	6.93	8.38
HUB (m)	2.12	2.63	2.21	2.04	2.54	3.17	2.55	2.00	2.01	2.64
CS (m^2)	20.31	23.83	20.84	28.83	20.3	25.67	22.51	21.76	21.62	22.8

* indicates marked linear changes of this parameter at urban–rural gradients. Forest types are: RF, roadside forest; AF, affiliated forest; LF, landscape and relaxation forest; EF, ecological and public welfare forest; and PF, production and management forest. Other abbreviations are: BD, soil bulk density; EC, soil electrical conductivity; DBH, tree diameter at breast height; TH, tree height; HUB, tree height under branch; and CS, tree crown size.

Soil properties showed different urban–rural patterns for different parameters (Table 2). Bulk density (BD) values did not demonstrate a monotonic trend. In the human disturbance time-related urban–rural gradients, BD ranged from 1.37 g/cm^3 to 1.39 g/cm^3, while the range was from 1.36 g/cm^3 to 1.38 g/cm^3 in the ring road-related urban–rural gradients. Soil pH values fluctuated up and down with the two urban–rural gradients. However, EC values showed a significant increasing trend in both urban–rural gradients (For different human disturbance times, $y = 0.709x + 101.808$, $R^2 = 0.976$, $p < 0.01$, and for different ring roads, $y = 14.68x + 84.12$, $R^2 = 0.882$, $p < 0.05$) (Table 2).

Tree size of DBH, TH, HUB and CS did not appear to have a monotonic change under the two urban–rural gradients. The largest DBH and TH were in the urban centre (114 years and 1st ring road), the largest HUB was in 60 years and the 1st ring road regions, and the biggest CS was located in 10 years and the 1st ring road regions (Table 2).

3.5. Inter-Correlations among SOCD, SR, Q$_{10}$ and TT

Figure 4 shows that SOCD is weakly but significantly related to SR and TT ($R^2 > 0.14$, $p < 0.001$) but not with Q$_{10}$ ($R^2 = 0.00$, $p > 0.05$), indicating that SOC accumulation was mainly due to an increase in TT. Soil basal respiration depended on SOCD and TT but had no relation with Q$_{10}$, whereas TT was negatively related with SR and Q$_{10}$ (Figure 4E,F). These results suggested SOC accumulation during urbanization might result from an increase in TT.
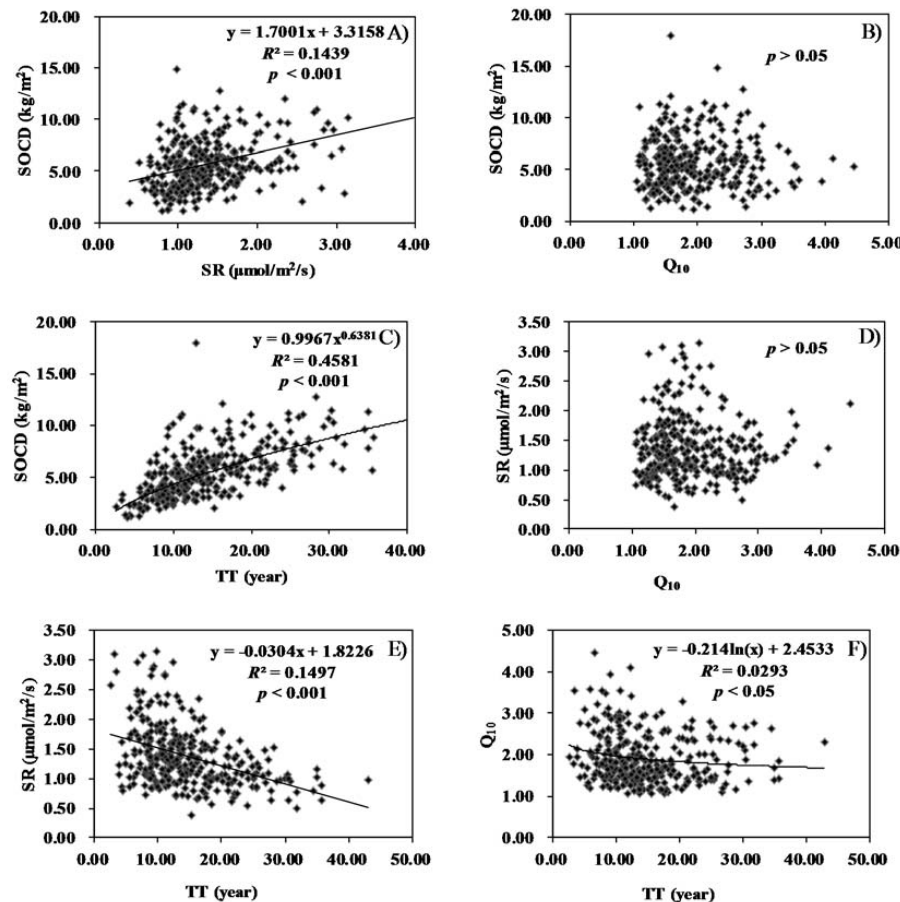
Figure 4. Correlations between (**A**) SOCD and SR; (**B**) SOCD and Q_{10}; (**C**) SOCD and TT; (**D**) SR and Q_{10}; (**E**) SR and TT and (**F**) Q_{10} and TT, for Changchun city of China. Notes: SOCD, soil organic carbon density; SR, soil basal respiration rate; and TT, turnover time.

3.6. Forest Types, Composition, Tree Sizes and Soil Properties and their Contributions to the Urban–Rural SOC Patterns

Pearson correlations were used to determine correlation coefficients for various factors (Table 3). The forest types and soil properties were significantly related with SOCD and Q_{10} variation, whereas SR was significantly associated with soil properties and tree size. TT was significantly related with forest type and species composition proportion as well as soil properties. Specifically, SOCD significantly increased with LF proportion and EC ($p < 0.01$). SR was significantly associated with EC ($p < 0.01$) and TH ($p < 0.05$). Q_{10} value was negatively associated with LF proportion and EC ($p < 0.01$). TT was related with LF proportion ($p < 0.01$), Pinaceae proportion ($p < 0.05$), conifer/broadleaf proportion ($p < 0.01$) and EC ($p < 0.05$). In other words, EC value was significantly related with all the four parameters, LF proportion had significant association with SOCD, Q_{10} and TT, tree species proportion was only associated with SR and TT, and TH only had influence on SR (Table 3).

Stepwise regression could explain 82.6–99.4% of variations of the 4 SOC-related parameters, and it also confirmed the findings in Pearson correlations (Table 4). Both EC and LF changes greatly affect the 4 SOC-related urban–rural patterns. With EC increases, increasing SOCD and SR, but decreasing Q_{10} values, were observed. With increases in LF proportion in different urban–rural gradients, increasing SOCD, SR and TT were found (Table 4). Standardized coefficients showed the relative contributions of the parameters to SOC-related parameters. EC's contribution was 2–6-fold higher than that in pH, DBH, Betulaceae and Rosaceae proportion, and LF proportion was the second contribution to SOC-related parameters (Table 4).

Table 3. Pearson correlations of SOCD, SR, Q_{10} and TT with forest types, tree species, soil properties and tree sizes, for Changchun city of China.

		SOCD	SR	Q_{10}	TT
	RF	−0.186	0.029	0.334	−0.534
	AF	0.280	0.093	−0.335	0.172
Forest types	LF	0.828 **	0.471	−0.722 **	0.866 **
	PF	−0.608	−0.426	0.617	−0.418
	EF	−0.519	−0.238	0.335	−0.472
	Betulaceae	−0.328	0.189	0.571	−0.504
	Aceraceae	0.379	0.210	−0.338	0.347
Compositional changes	Rosaceae	−0.193	−0.450	0.203	−0.120
	Pinaceae	0.367	0.055	−0.468	0.645 *
	Salicaceae	−0.569	−0.226	0.353	−0.481
	Ulmaceae	0.358	0.601	−0.449	−0.047
	Other SPP.	0.598	0.732	−0.440	0.159
Tree species	Conifer	0.348	0.024	−0.459	0.659 **
	Broadleaf	−0.348	−0.024	0.459	−0.659 **
Soil properties	BD	0.090	0.149	0.133	0.052
	pH	−0.084	0.166	0.122	−0.402
	EC	0.930 **	0.813 **	−0.903 **	0.637 *
	DBH	0.224	0.493	−0.051	0.088
Tree size properties	TH	0.499	0.739 *	−0.331	0.188
	HUB	0.223	0.121	−0.185	0.407
	CS	0.161	0.216	0.186	0.076

** indicates highly significant correlation and * indicates significant correlation. SOCD, soil organic carbon density; SR, soil basal respiration rate; and TT, turnover time. Forest types are: RF, roadside forest; AF, affiliated forest; LF, landscape and relaxation forest; EF, ecological and public welfare forest; and PF, production and management forest. Other abbreviations are: BD, soil bulk density; EC, soil electrical conductivity; DBH, tree diameter at breast height; TH, tree height; HUB, tree height under branch; and CS, tree crown size.

Table 4. Stepwise regressions of SOCD, SR, Q_{10}, TT and forest types, tree species, soil properties as well as tree sizes. Note: The parameter was included in the model when $p < 0.05$, while deleted when $p > 0.10$. SOCD, soil organic carbon density; SR, soil basal respiration rate; TT, turnover time. EC, soil electrical conductivity; LF, landscape and relaxation forest; and DBH, tree diameter at breast height.

Items	Model	Unstandardized Coefficients		Standardized Coefficients	*t*-Value	Sig.	R^2
		B	Std. Error	Beta			
SOCD	1 (Constant)	1.879	0.387		4.854	0.003	0.971
	EC	0.024	0.003	0.740	7.693	0.000	
	LF	2.433	0.589	0.387	4.128	0.006	
	Rosaceae	1.680	0.594	0.190	2.557	0.043	
SR	2 (Constant)	0.434	0.174		2.500	0.041	0.826
	EC	0.006	0.001	0.918	5.644	0.001	
	Betulaceae	2.042	0.791	0.420	2.581	0.036	
Q_{10}	3 (Constant)	−2.437	0.549		−4.435	0.007	0.994
	EC	−0.007	0.000	−1.250	−16.736	0.000	
	pH	0.546	0.068	0.540	8.015	0.000	
	DBH	0.049	0.005	0.430	10.522	0.000	
	LF	0.256	0.088	0.247	2.912	0.033	
TT	4 (Constant)	13.446	0.750		17.939	0.000	0.879
	LF	9.759	1.621	0.803	6.021	0.001	
	Betulaceae	−16.174	5.914	−0.365	−2.735	0.029	

3.7. Carbon Accumulated in Forest Soil Due to Urbanization

The annual net ecosystem exchange (NEE) is usually considered the carbon sink capacity of the studied ecosystem [35]. Average NEE of natural forests within the same region was 165 g m^{-2} year^{-1}, which was 36% smaller than the net primary production (NPP)-related C sinks. Urbanization-related C sequestration in soil was about 16% of the NEE (Figure 5A). At the city level, urban forest vegetation could fixate around 474,000 tons of C biomass [27], and the urbanization-induced SOC accumulation ranged from 61,000 tons (estimated from human disturbance time gradient) to 98,000 tons (estimated from the ring roads gradient), which is about 12.8–20.7% (16.8%, on average) of that sequestrated in urban forest biomass (Figure 5B).
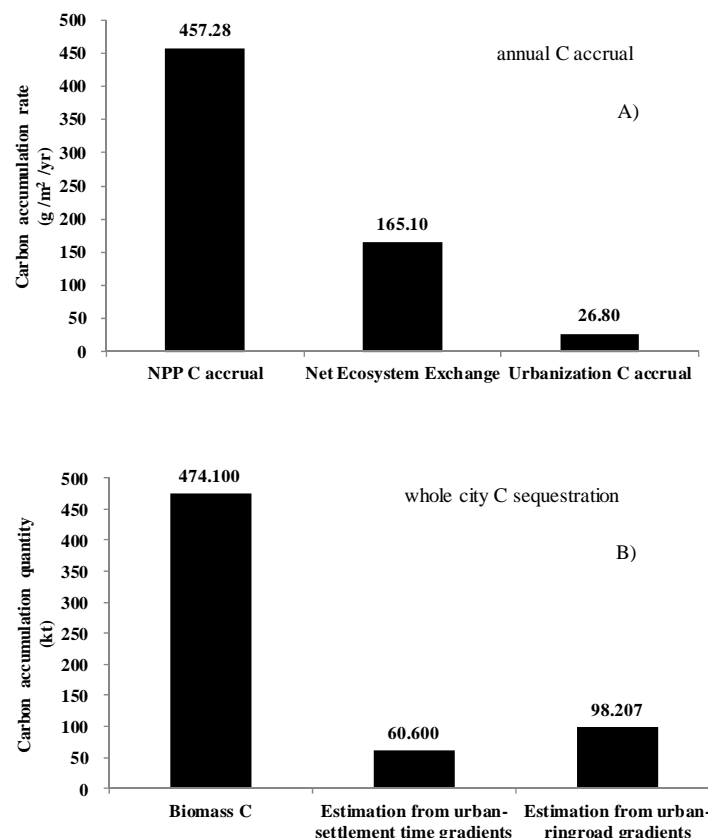
Figure 5. Comparison of urbanization-induced SOC accumulation, biomass C accumulation and ecosystem carbon sink capacity, for Changchun city of China. (**A**) Annual scale C-accrual of NPP, net ecosystem exchange and urbanization C accrual; (**B**) whole city C sequestration in biomass C and urbanization-related SOC accrual estimated from urban history gradients and ring road gradients. Notes: The NPP C accrual and biomass C were cited from reference 27, NEE was calculated by NPP and annual respiration, and urbanization C accrual value (1-m depth) was calculated as the 2-fold of 20-cm depth SOCD [37,38].

4. Discussion

4.1. Changchun SOCD and Its Related Character

Many studies have considered carbon storage capacity of forests or soil carbon in urban environments in relation to different land uses or land covers. The average SOCD in the topsoil of Changchun forests was 5.66 kg m^{-2} (0–20 cm), which was smaller than that found in Leicester (9.9 kg m^{-2}) (0–21 cm) [39] and Beijing (7.33 kg m^{-2}) (0–20 cm) [40] but larger than the average SOCD found in Guiyang (3.95 kg m^{-2}) (0–15 cm) [41], Changsha (3.87 kg m^{-2}) (0–15 cm) [42], Nanjing

(2.18 kg m^{-2}) (0–20 cm) [43] and Chuncheon (1.39 kg m^{-2}) (0–30 cm) [44]. One reason for such differences might be the relatively low temperature in Changchun [37]. This city is located in northeast China, at a higher latitude than the other cities, and its low temperatures might induce a slower decomposition rate of soil organic matter [45]. In addition, Changchun belongs to the north-eastern old industrial base, and its evolution and forest development were accompanied by heavy industrial development. This increased soil organic matter input from environmental pollution, including human-induced organic matter accumulation under trees cleaned by sanitation workers and drainage accumulation from the city [46,47], led to the down-regulation of SOC decomposition [45] for about 100 years. Similarly, Beijing, which is the largest city in China and presents heavy urbanization and industrialization, had the largest soil carbon content, almost identical to the value registered in Atlanta, United States (7.7 kg m^{-2}) [33].

The Q_{10} value obtained for Changchun (1.92 ± 0.03) was within the range reported for temperate forests (1.8–4.2) [48]. Mostly, excluding root respiration, natural forests have a larger Q_{10} value [34] than that registered in urban forests. Globally, the average Q_{10} value for soil respiration in urban forests, excluding root respiration, is above 3.5 [18], reaching only 2.81 in northeast China [27]. Thus, urban forests became less affected by temperature changes than natural forests. Contrary to the trend observed in SOCD, Q_{10} decreased with increasing urbanization (Figures 2C and 3C), indicating that forest soil basal respiration was less sensitive with temperature change under urbanization pressure, which might have led to SOCD accumulation (Figures 2A and 3A).

An average turnover time of 41.92 years has been reported for SOC in Chinese forests' topsoil [49]. In northeast China, a SOC turnover time of 13 years has been reported for the topsoil of temperate forests [50]. In the present study, the average SOC turnover time in the urban forest topsoil was 14.57 years, and it was much lower than average values determined for China but comparable to natural forests at the same latitude. However, our data were obtained under one settled condition in the laboratory, assumed as heterotrophic basal respiration, and the underestimation of respiration may lead to an overestimate of carbon turnover time. An increase in soil SOC accumulation and turnover time was evidenced by their positive correlations (Figure 4C). Thus, the increase in SOC turnover time observed from 1900 to 2014 indicated that the urbanization-induced SOC accumulation in soil was greater than the increase in basal respiration during the same period.

4.2. Characteristics of Urbanization and Carbon Accumulation Due to Urbanization

Some common metrics such as distance from urban core [9], urban settlement times [21] and the impervious surface area fraction [51] were also used to represent the urbanization gradients. However, in China, the different ring roads were mainly used to determine the urban core or outskirts for public awareness. In our study, we divided the urbanization gradients by different human disturbance times and different ring roads, and testified that the ring roads produce similar results as the human disturbance times on forest C dynamics. This is helpful for citizens to understand the urbanization effects on forest soil C variations, and makes it easier to obey the government regulations about C cycles.

Although many previous studies considered urbanized SOC data, some reported high SOC content in downtown or old urban regions, while few of them reported the SOC accumulation rate. As in Chongqing, Southwest China, the areas developed from 2001 to 2010 had a lower SOCD than the areas built before 1988 [52] and in Shanghai, Southeast China, older parks had higher SOCD (201 t ha^{-1}) than younger parks (107 t ha^{-1}) [53]. Forest SOCD decreased from 4.24 kg C m^{-2} to 3.99 kg C m^{-2} from urban to suburban Boston, United States [9], and in west Georgia (United States), SOCD in 1974, 1980, and 1990 was 5.487 kg C m^{-2}, 5.492 kg C m^{-2}, and 5.518 kg C m^{-2}, respectively [8]. In Harbin city, forest soil was accumulating at a speed of 15.4 g C m^{-2} year^{-1} [21]. Our study reported an SOC increasing rate of 13.4 g C m^{-2} year^{-1}, which was much lower than Harbin city.

In addition to the increase in total SOC, old urbanized regions had more temperature-stabled SOC with longer turnover times than in new urbanized regions. The carbon stability calculated for

the 1st ring road was 6%, 7%, 13%, and 19% higher than that calculated for the 2nd, 3rd, 4th, and 5th ring roads, respectively. Carbon stability calculated for the human disturbance time of 114 years was 7%, 13%, 18%, and 15% higher than that calculated for 60, 24, 10, and 0 years, respectively. Therefore, SOC sequestration capacity might be even larger than expected in the above estimations, due to increasing SOC stability and longer SOC turnover time. The lower Q_{10} value with urbanization meant a higher temperature stability and a lower soil basal respiration [54]. Therefore, greater carbon accumulation, longer carbon turnover time, and more stable carbon sequestration are the main features of urbanization-induced forest SOC accumulation.

4.3. Possible Reasons for the Urbanization-Induced Forest SOC Changes

The most important reasons for SOC accumulation under urbanization were the forest type-related land use alternations and EC-related soil property changes, and this is an important finding of this paper. It was reported that the forest floor C stocks are directly affected by litterfall C inputs [19]. Compared with other forest types, LF is mainly located in the semi-natural environments (such as public parks, forest parks, historic sites, and scenic areas), and the larger litterfall in LF might increase the C inputs over other forest types (RF, AF, PF and EF) for their large areas where people cannot easily disturb. Also, human activities in LF potentially increase human-related C (such as the food and rubbish people bring in) inputs into soils, as these places are attractive sites for sightseeing and physical activities [46]. Therefore, the close correlations between LF proportion and SOC-related parameters indicates that land uses of LF are a driver of SOC accumulation as shown in urban–rural gradients (Tables 2 and 3). EC value was positively associated with SOCD and the changing trend was similar to SOCD (Tables 2 and 3). EC is a proxy for soil salinity [22] and a decrease in salinity would improve the accessibility of soil organic matter to the soil microbial community [55]. In Northeast China, heavy snow in winter is usually accompanied with large amounts of snow-melting salt utilization. This salt utilization probably increases soil EC [56], and it is likely a pattern that urban central regions had more utilization of these salts. Therefore, the high EC value in urban centres was another driver of SOC accumulation.

Our study also showed that only the proportion of Pinaceae and conifer/broadleaf trees had associations with TT, and the compositional changes had marginal associations with SOCD, basal respiration and Q_{10} (Table 3), and this is different from those in non-urban sites. In non-urban forests, species differences were important drivers for SOC changes [19]. Conifer forests showed much lower SOC accumulation capacity than broadleaf forests in Natural reserves in NE China [24]. This kind of leaf phenological differences-related SOC changes did not contribute to urban–rural SOC patterns, which were manifested in this study too (Table 3). During urbanization processes, heavy human disturbance including litter removal, watering and fertilization, etc., are possibly changing the natural-based patterns. These changes may include low quality of litter within or near urban cores [57], microbial diversity in rural, suburban, and urban stands contributing to organic material decomposition [23,57], microclimate differences, nutrient inputs, and changes in soil fauna [58]. Some more detailed studies related to inter-species differences should be done both in urban and natural regions to identify underlying contributions of different species to soil conditions and processes.

Understanding the potential factors affecting urban forest SOC accumulation under urbanization, serves to improve the capacity of carbon sinks of urban forests in the future. For example, an effective method was to increase the LF proportion in an urban region, although such activity is difficult in the city owing to limited green space available in urban areas. In Changchun city, the green space coverage decreased from 45.42% to 30.65% from 2006 to 2014 [59]. Secondly, chemical snow-melting salt utilization could enhance the salinity of soil, with many disadvantages on surface water, ground water, vegetation and animals [56]. However, SOC accumulation should be one good effect for such salt utilization, which has been shown by the positive relations between EC and SOCD in this paper. Finally, urbanization-induced forest SOC accumulation should be fully considered in terrestrial C

balance analysis, given that the background of urbanization has become the first driver of land use changes in today's world [1].

Some research uncertainty in this study should be pointed out, too. Firstly, laboratory-based basal respiration data may be dramatically different from those in field, although this kind of laboratory respiration measured is used as a routine method for basal respiration measurement [32]. SOC/respiration ratio is often used as an indicator of SOC turnover in instant measurements. In this paper, the scale-up from laboratory measurement to whole-year soil respiration, as well as SOC turnover time, might be different from some exact measurements, such as isotope measurements, although the patterns at urban–rural gradients in soil respiration, Q_{10} and TT should be reliable in this paper. During field surveys, in situ soil respiration was not fully distinguishable between autotrophic and heterotrophic sources in such a large-scale survey, and ensuring the same environments (temperature and moisture, two important factors controlling respiration capacity) and field methods (such as the stretched-box method), were not possible in urban environments [12]. The laboratory incubation method should be the optimal way to measure the respiration differences among the 306 samples in the same environment, and also Q_{10} values. Secondly, land use changes were not clear during the 100-year urbanization process. Our study manifested that land use alternations (such as LF proportion) are an important reason for the urbanized SOC pattern. The original land use in this region before urbanization was grassland/pasture. Owing to frequent disturbance in urban regions, the previous land-uses in some studied forests in this paper (such as roadside forest) were not recorded clearly. This may increase the uncertainty of this paper too, as for example, whether old city forest SOC increases or outer new city region SOC decreases, are the main contributors to the urban–rural pattern of carbon dynamics.

5. Conclusions

Our study provides a case study about the influence of urbanization on forest SOC sequestration, basal respiration, temperature stability and carbon turnover time in Changchun, a medium-sized mid-latitude city in Northeast China. Based on the field survey and laboratory experiments, we concluded that the urbanization process had significant influence on SOCD, SR, Q_{10} and TT, and we confirmed the hypothesis that the ring road-related urban–rural gradient had the same effect on SOC-related parameters as the human disturbance time. Driven by urbanization, forest SOC has accumulated at a speed of 13.4 g C m^{-2} year^{-1}, Q_{10} has decreased 0.076 year^{-1}, and SOC turnover time has increased 0.041 year^{-1} since 1900. Increases in LF proportions, as well as increases in soil EC values, are mainly responsible for these urbanization-induced SOC changes. Scaling-up of Changchun city data highlights the importance of forest SOC accumulation in terrestrial C balance; therefore, we argue that it is essential to consider the urban–rural gradient into carbon sink capacity research. These findings in this paper would help us to better understand the forest soil carbon budget under global change and its feedback on the environment.

Author Contributions: X.H. and W.W. designed the research, provide research fund and discussion on the result. C.Z., W.Z., L.X. and B.Z. collected field data, analyzed the soil sample and performed all the experiments. C.Z. analyzed the data, prepared figures and wrote the manuscript. W.W. and X.H. revised the manuscript, and supervised on data analysis.

References

1. Hutyra, L.R.; Duren, R.; Gurney, K.R.; Grimm, N.; Kort, E.A.; Larson, E.; Shrestha, G. Urbanization and the carbon cycle: Current capabilities and research outlook from the natural sciences perspective. *Earth's Future* **2014**, *2*, 473–495. [CrossRef]

2. Yue, W. *Research on China's New Urbanization Development*; Wuhan University: Wuhan, China, 2013.

3. Pouyat, R.V.; Yesilonis, I.D.; Nowak, D.J. Carbon storage by urban soils in the United States. *J. Environ. Qual.* **2006**, *35*, 1566–1575. [CrossRef] [PubMed]

4. Schlesinger, W.H.; Andrews, J.A. Soil respiration and the global carbon cycle. *Biogeochemistry* **2000**, *48*, 7–20. [CrossRef]

5. Mcdonnell, M.J.; Pickett, S.T.A. Ecosystem Structure and Function along Urban-Rural Gradients: An Unexploited Opportunity for Ecology. *Ecology* **1990**, *71*, 1232–1237. [CrossRef]

6. Clergeau, P.; Falardeau, G. Bird abundance and diversity along an urban-rural gradient: A comparative study between two cities on different continents. *Condor* **1998**, *100*, 413–425. [CrossRef]

7. Pouyat, V.R.; Mcdonnell, J.M. Heavy metal accumulations in forest soils along an urban–rural gradient in Southeastern New York, USA. *Water Air Soil Pollut.* **1991**, *57–58*, 797–807. [CrossRef]

8. Zhang, C.; Tian, H.; Pan, S.; Liu, M.; Lockaby, G.; Schilling, B.E.; Stanturf, J. Effects of Forest Regrowth and Urbanization on Ecosystem Carbon Storage in a Rural–Urban Gradient in the Southeastern United States. *Ecosystems* **2007**, *11*, 1211–1222. [CrossRef]

9. Rao, P.; Hutyra, R.L.; Raciti, M.S.; Finzi, C.A. Field and remotely sensed measures of soil and vegetation carbon and nitrogen across an urbanization gradient in the Boston metropolitan area. *Urban Ecosyst.* **2013**, *16*, 593–616. [CrossRef]

10. Wei, Z.; Wu, S.; Yan, X.; Zhou, S. Density and stability of soil organic carbon beneath impervious surfaces in urban areas. *PLoS ONE* **2014**, *9*, e109380. [CrossRef] [PubMed]

11. Wang, J.W.; Wang, M.H.; Zu, Y.G.; Li, X.Y.; Takayoshi, K. Characteristics of the temperature coefficient, Q_{10}, for the respiration of non-photosynthetic organs and soils of forest ecosystems. *Front. For. China* **2006**, *1*, 125–135. [CrossRef]

12. Wang, J.W.; Zu, G.Y.; Wang, M.H.; Hirano, T.; Takagi, K.; Sasa, K.; Koike, T. Effect of collar insertion on soil respiration in a larch forest measured with a LI-6400 soil CO_2 flux system. *J. For. Res.* **2005**, *10*, 57–60. [CrossRef]

13. Bae, J.; Ryu, Y. Land use and land cover changes explain spatial and temporal variations of the soil organic carbon stocks in a constructed urban park. *Landsc. Urban Plan.* **2015**, *136*, 57–67. [CrossRef]

14. Rossiter, D.G. Classification of Urban and Industrial Soils in the World Reference Base for Soil Resources (5 pp). *J. Soils Sediments* **2007**, *7*, 96–100. [CrossRef]

15. Rawlins, G.B.; Vane, H.C.; Kim, W.A.; Tye, M.A.; Kemp, J.S.; Bellamy, H.P. Methods for estimating types of soil organic carbon and their application to surveys of UK urban areas. *Soil Use Manag.* **2008**, *24*, 47–59. [CrossRef]

16. Nowak, D.J.; Crane, E.D. Carbon storage and sequestration by urban trees in the USA. *Environ. Pollut.* **2002**, *116*, 381–389. [CrossRef]

17. Kahan, A.; Currie, W.; Brown, D. Nitrogen and Carbon Biogeochemistry in Forest Sites along an Indirect Urban–Rural Gradient in Southeastern Michigan. *Forests* **2014**, *5*, 643–665. [CrossRef]

18. Chi, Z.; Tian, H.; Chen, G.; Chappelka, A.; Xu, X.; Wei, R.; Hui, D.; Liu, M.; Lu, C.; Pan, S. Impacts of urbanization on carbon balance in terrestrial ecosystems of the Southern United States. *Environ. Pollut.* **2012**, *164*, 89–101.

19. Lars, V.; Nicholas, C.; Bjarni, S.D.; Per, G. Do tree species influence soil carbon stocks in temperate and boreal forests? *For. Ecol. Manag.* **2013**, *309*, 4–18.

20. He, X.; Liu, C.; Chen, W.; Guan, Z.; Zhao, G. Discussion on urban forest classification. *Chin. J. Ecol.* **2004**, *23*, 175–178.

21. Lv, H.; Wang, W.; He, X.; Xiao, L.; Zhou, W.; Zhang, B. Quantifying Tree and Soil Carbon Stocks in a Temperate Urban Forest in Northeast China. *Forests* **2016**, *7*, 1–18. [CrossRef]

22. Wang, J.W.; Qiu, L.; Zu, Y.; Su, D.; An, J.; Wang, H.; Zheng, G.; Sun, W.; Chen, X. Changes in soil organic carbon, nitrogen, pH and bulk density with the development of larch (*Larix gmelinii*) plantations in China. *Glob. Chang. Biol.* **2011**, *17*, 2657–2676.

23. Li, Y.; Wang, H.; Wang, W.; Yang, L.; Zu, Y. Ectomycorrhizal influence on particle size, surface structure, mineral crystallinity, functional groups, and elemental composition of soil colloids from different soil origins. *Sci. World J.* **2013**, *2013*, 698752. [CrossRef] [PubMed]

24. Ming, Y.Y.; Juan, W.; Man, H.X.; Xin, Z.T.; Rong, S.L.; Osbert, J.S. Relating microbial community structure to functioning in forest soil organic carbon transformation and turnover. *Ecol. Evol.* **2014**, *4*, 633–647.

25. Wang, H.; Wang, W. Chang, Sampling method and tree-age affect soil organic C and N contents in larch plantations. *Forests* **2017**, *8*, 1–15. [CrossRef]

26. Ren, Z.; He, X.; Zheng, H.; Zhang, D.; Yu, X.; Shen, G.; Guo, R. Estimation of the Relationship between Urban Park Characteristics and Park Cool Island Intensity by Remote Sensing Data and Field Measurement. *Forests* **2013**, *4*, 868–886. [CrossRef]

27. Zhang, D.; Zheng, H.; Ren, Z.; Zhai, C.; Shen, G.; Mao, Z.; Wang, P.; He, X. Effects of forest type and urbanization on carbon storage of urban forests in Changchun, Northeast China. *Chin. Geogr. Sci.* **2015**, *25*, 147–158. [CrossRef]

28. Kuang, W.; Zhang, S.; Zhang, Y.; Sheng, Y. Analysis of urban land utilization spatial expansion mechanism in Changchun city since 1900. *ACTA Geogr. Sin.* **2005**, *60*, 841–850.

29. Huang, C.D.; Su, M.Z.; Zhang, Z.R.; Koh, P.L. Degree of urbanization influences the persistence of *Dorytomus* weevils (Coleoptera: Curculionoidae) in Beijing, China. *Landsc. Urban Plan.* **2010**, *96*, 163–171. [CrossRef]

30. Nowak, J.D.; Crane, D.E.; Stevens, C.J. *The Urban Forest Effects (UFORE) Model: Field Data Collection Manual*; US Department of Agriculture Forest Service, Northeastern Research Station: New York, NY, USA, 2003.

31. Bao, D.S. *The Method of the Soil and Agriculture Chemical Analysis*; China Agriculture Press: Beijing, China, 2000.

32. Pouyat, R.; Groffman, P.; Yesilonis, I.; Hernandez, L. Soil carbon pools and fluxes in urban ecosystems. *Environ. Pollut.* **2002**, *116*, 107–118. [CrossRef]

33. Plante, F.A.; Conant, T.R.; Carlson, J.; Greenwood, R.; Shulman, M.J.; Haddix, L.M.; Paul, A.E. Decomposition temperature sensitivity of isolated soil organic matter fractions. *Soil Biol. Biochem.* **2010**, *42*, 1991–1996. [CrossRef]

34. Zu, Y.; Wang, W.; Wang, H.; Liu, W.; Cui, S.; Koike, T. Soil CO_2 efflux, carbon dynamics, and change in thermal conditions from contrasting clear-cut sites during natural restoration and uncut larch forests in northeastern China. *Clim. Chang.* **2009**, *96*, 137–159. [CrossRef]

35. Carvalhais, N.; Forkel, M.; Khomik, M.; Bellarby, J.; Jung, M.; Migliavacca, M.; Mu, M.; Saatchi, S.; Santoro, M.; Thurner, M.; et al. Global covariation of carbon turnover times with climate in terrestrial ecosystems. *Nature* **2014**, *514*, 213–217. [CrossRef] [PubMed]

36. Cai, H.; Di, X.; Chang, X.S.; Wang, C.; Shi, B.; Geng, P.; Jin, G. Carbon storage, net primary production, and net ecosystem production in four major temperate forest types in northeastern China. *Can. J. For. Res.* **2016**, *46*, 143–151. [CrossRef]

37. Mao, H.D.; Wang, M.Z.; Li, L.; Miao, H.Z.; Ma, H.W.; Song, C.C.; Ren, Y.C.; Jia, M.M. Soil organic carbon in the Sanjiang Plain of China: Storage, distribution and controlling factors. *Biogeosciences* **2015**, *12*, 1635–1645. [CrossRef]

38. Wang, S.; Huang, M.; Shao, X.; Mickler, A.R.; Li, K.; Ji, J. Vertical Distribution of Soil Organic Carbon in China. *Environ. Manag.* **2004**, *33*, S201–S209. [CrossRef]

39. Edmondson, L.J.; Davies, G.Z.; McCormack, A.S.; Gaston, J.K.; Leake, R.J. Land-cover effects on soil organic carbon stocks in a European city. *Sci. Total Environ.* **2014**, *472*, 444–453. [CrossRef] [PubMed]

40. Luo, S.; Mao, Q.; Ma, K. Comparison on soil carbon stocks between urban and suburban topsoil in Beijing, China. *Chin. Geogr. Sci.* **2014**, *24*, 551–561. [CrossRef]

41. Wang, X. *Study of Biomass and Carbon Sequestration on Urban Forests in Karst Landform*; Central South University of Forestry & Technology: Changsha, China, 2011.

42. Gao, S.; Tian, D.; Yan, W.; Fang, X.; Xiang, W.; Liang, X. Characteristics of soil physicochemical property and its carbon storage in urban forest plantation of Changsha city. *J. Cent. South Univ. For. Technol.* **2010**, *30*, 16–22.

43. Wang, Z.; Liu, H.; Guan, Q.; Wang, X.; Hao, J.; Ling, N.; Shi, C. Carbon storage and density of urban forest ecosystems in Nanjing. *J. Nanjing For. Univ. (Nat. Sci. Ed.)* **2011**, *35*, 18–22.

44. Jo, H. Impacts of urban greenspace on offsetting carbon emissions for middle Korea. *J. Environ. Manag.* **2002**, *64*, 115–126. [CrossRef]

45. Yang, Y.; Fang, J.; Tang, Y.; Ji, C.; Zheng, C.; He, J.; Zhu, B. Storage, patterns and controls of soil organic carbon in the Tibetan grasslands. *Glob. Chang. Biol.* **2008**, *14*, 1592–1599. [CrossRef]

46. Bian, Z.; Wang, Q. Study on urban park soil nutrients in Shenyang City's green areas. *J. Soil Sci.* **2003**, *34*, 284–290.

47. Zhang, M.; Zhou, C. Characterization of Organic Matter Accumulated in Urban Soils in the Hangzhou City. *Chin. J. Soil Sci.* **2006**, *37*, 19–21.

48. Xu, M.; Qi, Y. Spatial and seasonal variations of Q_{10} determined by soil respiration measurements at a Sierra Nevadan forest. Glob. Bolgeochem. *Cycles* **2001**, *15*, 687–696. [CrossRef]

49. Zhou, T.; Shi, P.; Jia, G.; Li, X.; Luo, Y. Spatial pattern of forest ecosystem carbon turnover time of China. *Sci. China* **2010**, *40*, 632–644.

50. Yang, J.; Wang, C. Soil carbon storage and flux of temperate forest ecosystems in northeastern China. *ACTA Ecol. Sin.* **2005**, *25*, 2875–2882.

51. Berland, A. Long-term urbanization effects on tree canopy cover along an urban-rural gradient. *Urban Ecosyst.* **2012**, *15*, 721–738. [CrossRef]

52. Liu, Y.; Wang, C.; Yue, W.; Hu, Y. Storage and density of soil organic carbon in urban topsoil of hilly cities: A case study of Chongqing Municipality of China. *Chin. Geogr. Sci.* **2013**, *23*, 26–34. [CrossRef]

53. Wang, Z.; Cui, X.; Yin, S.; Shen, G.; Han, Y.; Liu, C. Characteristics of carbon storage in Shanghai's urban forest. *Chin. Sci. Bull.* **2012**, *58*, 1130–1138. [CrossRef]

54. Shi, B.; Gao, W.; Jin, G. Effects on rhizospheric and heterotrophic respiration of conversion from primary forest to secondary forest and plantations in northeast China. *Eur. J. Soil Biol.* **2015**, *66*, 11–18. [CrossRef]

55. Yuan, D.G.; Zhang, G.L. Vertical Distribution Characterization of Electrical Conductivity of Urban Soil under Different Land Use Type. *J. Soil Water Conserv.* **2010**, *24*, 171–176.

56. Yan, X.; Li, Y.F.; Liu, W.T.; Zhang, Y.; Ma, P.X.; Wang, J.X. Effects of deicing chemicals on ecological environment. *Chin. J. Ecol.* **2007**, *13*, 2209–2214.

57. Carreiro, M.M.; Howe, K.; Parkhurst, F.D.; Pouyat, V.R. Variation in quality and decomposability of red oak leaf litter. *Biol. Fertil. Soils* **1999**, *30*, 258–268. [CrossRef]

58. Trumbore, E.S. Potential responses of soil organic carbon to global. *Proc. Natl. Acad. Sci. USA* **1997**, *94*, 8284–8291. [CrossRef] [PubMed]

59. Tang, Z.; Zheng, F.H.; Ren, B.Z.; Cui, X.M.; He, Y.X. Spatial and temporal changes to urban surface thermal landscape patterns: A case study of Changchun City. *Acta Ecol. Sin.* **2017**, *3710*, 1–10.